Electronic Supplementary Information

Ultrathin Carbon-coated FeS_2 Nanooctahedra for Sodium Storage with Long Cycle Stability

Experimental Section

1. Preparation of neat FeS_2 nanooctahedra

Typically, uniform FeS_2 nanooctahedra samples were prepared by a solvothermal reaction. Firstly, 1.05 g of polyvinyl pyrrolidone (PVP) and 0.556 g of $FeSO_4 \cdot 4H_2O$ were dissolved in 60 mL absolute ethylene glycol to get a transparent solution after stirring for 1h. Then 10 mL NaOH solution (1 M) and 0.4 g sublimed sulfur powder were respectively added to the solution and stirred continuously for 1h. Afterward, the as-obtained black solution was transferred into a 100 mL Teflon-lined scaled autoclave, sealed and heated at 180 ºC for 12 h under pressure of approximately 2 MPa. Eventually the final product was centrifuged, washed by deionized water and absolute ethyl alcohol three times, respectively, and collected after drying at 110 ºC for 10 h in a vacuum oven.

2. Preparation of porous ultrathin carbon-coated FeS_2@C nanooctahedra

In brief, 0.2 g of the as-synthesized FeS_2 nanooctahedra and 0.33 g of glucose were added into a 100 mL Teflon-lined scaled autoclave containing 60 mL deionized water and heated at 190 ºC for 10 h under pressure of approximately 1.8 MPa. Similarly, the prepared composites were centrifuged, washed by deionized water and absolute ethyl alcohol three times, and then further dried in a vacuum oven at 110 ºC for 10 h. Subsequently, before pickled by HCl (6 M) the composites were annealed at 500 ºC in a N_2 flow for 45 min to obtain the ultimate product (FeS_2@C) with porosity and enhanced conductivity.

CAUTION! Only professional and technical personnel or one who have accepted special training will be allowed to do autoclave experiments. Furthermore, before operating the experiment, please carefully check whether there are cracks and deformation in the autoclave. When autoclave experiment is scaled up, some safety precautions such as open and ventilated environment, temperature and pressure alarm apparatus, especially anti-explosion reactor should be taken into account.

Material characterization

The morphologies and structures of the as-prepared samples were characterized by field emission scanning electron microscopy (FESEM, JEOL JSM-6490LV) images operated at 10 kV and transmission electron microscopy (TEM, JEOL JEM-2100) images and high-resolution TEM (HRTEM) images. The X-ray powder diffraction (XRD) patterns were examined on a Bruker D8 advance diffractometer with Cu Kα radiation (λ = 0.15405 nm). Raman spectra were recorded on a LabRAM HR Evolution Raman spectrometer system (HORIBA Scientific) with an excitation wavelength of 532 nm. Furthermore, the exact surface areas and pore size distribution of the samples were obtained on Belsorp-mini II (BEL Japan, Inc.) via the Brunauer-Emmett-Teller method from the N_2 adsorption-desorption isotherms which were collected at 77 K. The X-ray photoelectron spectroscopy (XPS) analysis was carried out on an ESCALAB 250Xi spectrometer (Thermo Scientific). Thermo-gravimetric (TG) analysis of the products was performed by Netzsch STA 449 F3 Jupiter analyzer in air flow at a heating rate of 5 °C/min. For ex situ SEM and TEM observation, the cell at fully charge state was disassembled in Ar-filled glove box. The electrode paste was repeatedly rinsed with diethylene glycol dimethyl ether solvent and vaccum-dried at 100 ºC for 2 h. Afterward, the active materials were carefully made into corresponding samples, quickly moved into test platforms under protection of inert atmosphere. The samples were protected in the glove box with Ar atmosphere away from air and moisture.

Electrochemical measurements

Electrochemical tests were conducted by self-assembled CR2032 coin-type cells with circulated Na foil disk and a glass fiber porous film as the counter electrode and separator, respectively. The working electrodes were constructed by mixing 90 wt% active material (FeS_2 nanooctahedras or FeS_2@C octahedral nanocomposites), 5 wt% Super P and 5 wt% polyvinylidene difluoride (PVDF) dissolved in *N*-methylpyrrolidinone (NMP). After uniformly mixing, the homogeneous slurry was

smeared onto a copper foil of 14 mm diameter and dried at 110 ºC for 10 h in vacuum oven. Then the films were pressed under a pressure of 5 MPa. The loading of the active material in the electrode was ~2.0 mg cm^{-2}. The coin cells were assembled in a glove box filled with highly pure argon gas with moisture content and oxygen level below 1 ppm. The electrolyte solution was 1 M sodium trifluomethanesulfonate ($NaSO_3CF_3$) dissolved in diethylene glycol dimethyl ether (DEGDME). The galvanostatic tests were conducted on a battery testing system (Shenzhen Neware battery Co. Ltd, China) with the voltage range of 0.8–2.8 V (*vs*. Na^+/Na) at room temperature (298 K). Cyclic voltammograms (CV) were cycled between 0.8–2.8 V at a scan rate of 0.1 mV s^{-1} and electrochemical impedance spectroscopy (EIS) was conducted on Autolab PGSTAT302N electrochemical workstation. The perturbation voltage of EIS tests was 5 mV and the frequency range from 100 mHz to 100 kHz.

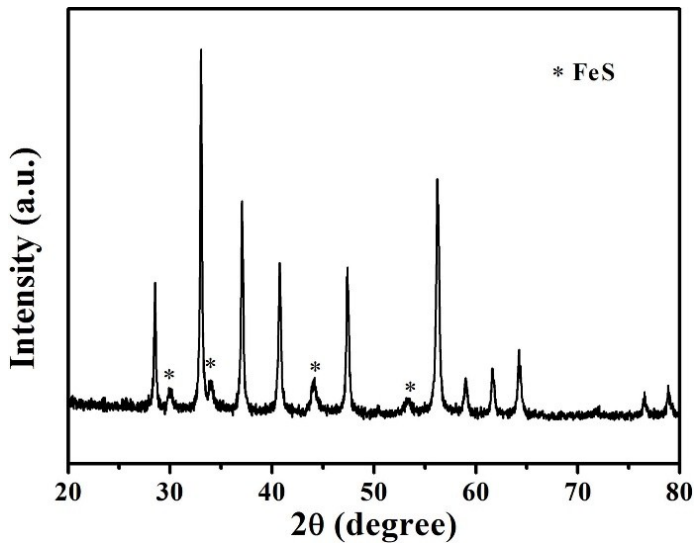

Figure S1. XRD pattern of FeS_2@FeS@C intermediate after annealing without pickled by HCl solution.

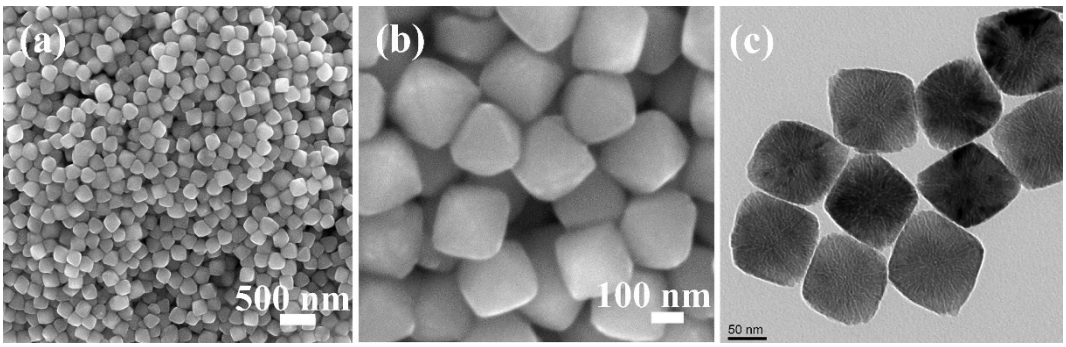

Figure S2. (a, b) SEM and TEM image of (c) neat FeS_2 nanooctahedra.

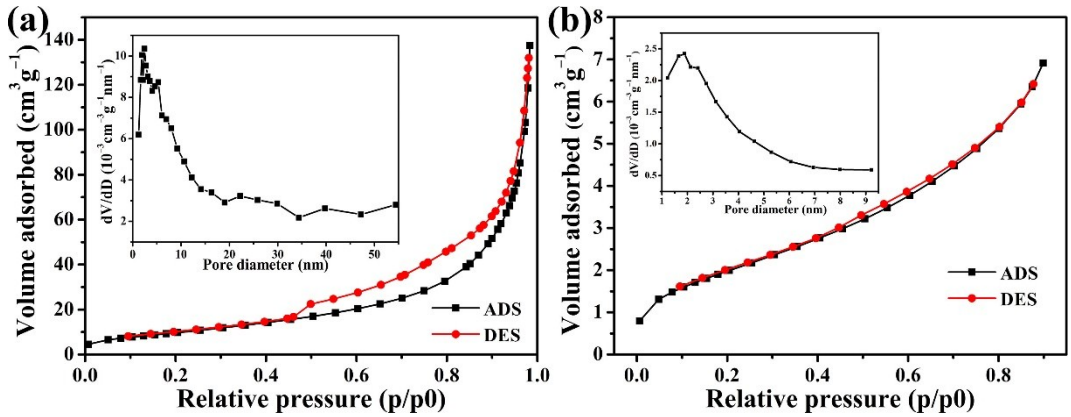

Figure S3. The isotherms of N_2 adsorption/desorption and the pore size distribution (the inset) of (a) FeS_2@C nanooctahedra and (b) neat FeS_2 nanooctahedra.

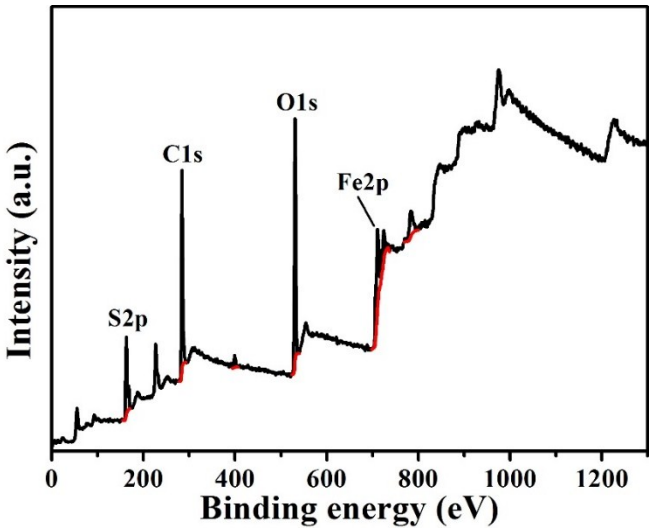

Figure S4. The survey XPS spectrum of FeS_2@C nanooctahedra.

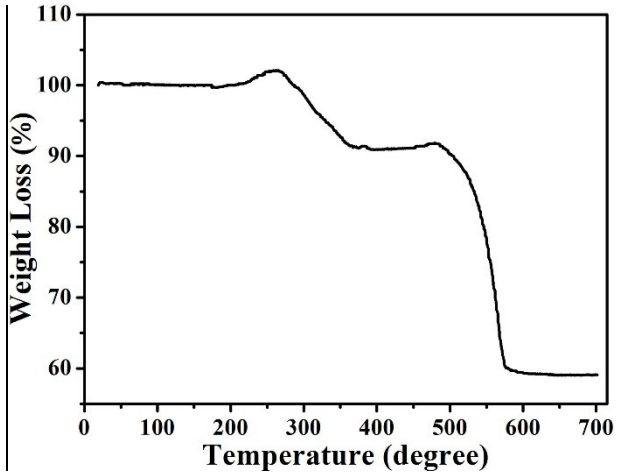

Figure S5. TG curve of FeS_2@C nanooctahedra in air atmosphere.

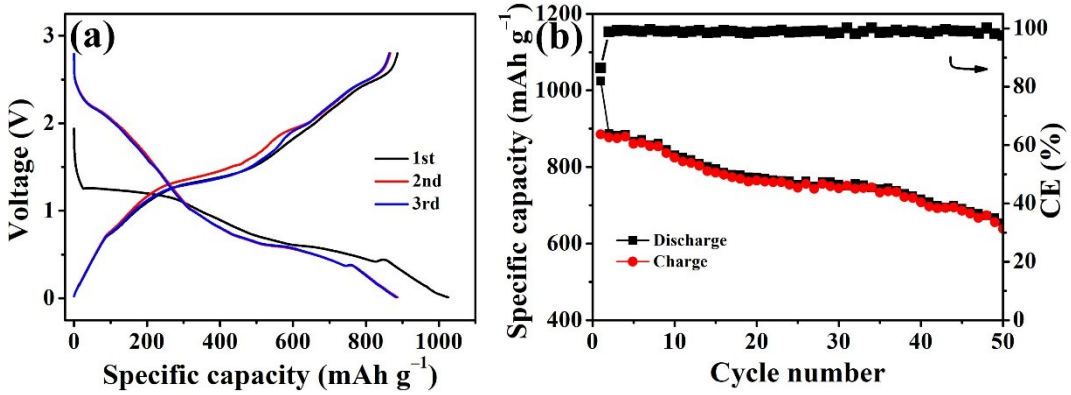

Figure S6. The discharge and charge curves of FeS_2@C cathode for the first three cycles between 0.01–2.8 V at 0.1C; (c) cycling performance and CE of FeS_2@C at the rate of 0.1C.

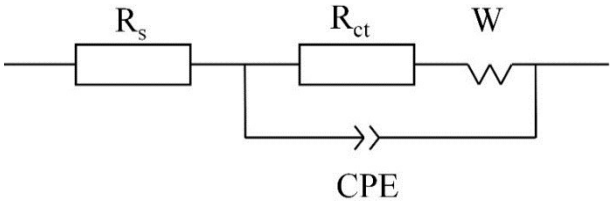

Figure S7. The parallel equivalent circuit model of EIS of both FeS_2 and FeS_2@C electrodes after 50 cycling.

After 50 cycling, charge transfer resistance Rct of the FeS_2@C electrode is significantly lower than that of the FeS_2 electrode (see Table S1), further demonstrating that the porous ultrathin-carbon-coated pyrite FeS_2@C nanooctahedra reduces the internal resistance.

Table S1 Summary of EIS fitting results.

Sample	R_s (Ω)	R_{ct} (Ω)	W (Ω)
FeS_2 electrode	8.211	42.8	0.44
FeS_2@C electrode	7.955	4.683	0.372

Table S2 Comparison of the electrochemical performance of the herein presented carbon-coated pyrite FeS_2@C nanooctahedra with previously reported results obtained with FeS_2-based electrodes in SIBs.

Types of materials	Long cycling performance	Rate capability	Voltage range	Ref.

Pyrite FeS_2	90% capacity retention after 20000 cycles at 1 A g^{-1}	170 mA h g^{-1} at 20 A g^{-1}	0.8–3.0 V	1
FeS_2@C yolk-shell nanobox	330 mA h g^{-1} after 800 cycles at 2 A g^{-1}	403 mA h g^{-1} at 5 A g^{-1}	0.1–2.0 V	2
Pyrite (FeS_2) NCs	500 mA h g^{-1} after 400 cycles at 1 A g^{-1}	600 mA h g^{-1} at 5000 mA g^{-1}	0.02–2.5 V	3
FeS_2/CNT-NN	309 mA h g^{-1} after 1800 cycles at 1 A g^{-1}	340 mA h g^{-1} at 22 A g^{-1}	0.8–3.0 V	4
FeS_2 anode	87.8% capacity retention after 800 cycles at 200 mA g^{-1}	323 mA h g^{-1} at 5 A g^{-1}	0.5−3.0 V	5
Cobalt-doped FeS_2 nanospheres	220 mA h g^{-1} after 5000 cycles at 2 A g^{-1}	172 mA h g^{-1} even at 20 A g^{-1}	0.8–2.9 V	6
FeS_2/rGO-A	58.03% capacity retention after 800 cycles at 1C	370 mA h g^{-1} at 0.1C	0.8–2.8 V	7
FeS_2@C nanorods	99% capacity retention after 9000 cycles at 10 A g^{-1}	140 mA h g^{-1} at 20 A g^{-1}	0.8-3.0 V,	8
FeS_2@rGO	240.5 mA h g^{-1} after 250 cycles at 0.5C	303.8 mA h g^{-1} at 0.1C	0.8–3.0 V	9
FeS_2@C nanooctahedra	89% capacity retention after 2000 cycles at 10C	417 mA h g^{-1} at 0.1C	0.8–2.8 V	**Present work**

References

1 Z. Hu, Z. Zhu, F. Cheng, K. Zhang, J. Wang, C. Chen and J. Chen, *Energy Environ. Sci.*, 2015, **8**, 1309-1316.·

2 Z. Liu, T. Lu, T. Song, X.-Y. Yu, X. W. Lou and U. Paik, *Energy Environ. Sci.*, 2017, **10**, 1576-1580.·

3 M. Walter, T. Zund and M. V. Kovalenko, *Nanoscale*, 2015, **7**, 9158-9163.·

4 Y. Chen, X. Hu, B. Evanko, X. Sun, X. Li, T. Hou, S. Cai, C. Zheng, W. Hu and G. D. Stucky, *Nano Energy*, 2018, **46**, 117-127.·

5 K. Chen, W. Zhang, L. Xue, W. Chen, X. Xiang, M. Wan and Y. Huang, *ACS Appl. Mater. Interfaces*, 2017, **9**, 1536-1541.·

6 K. Zhang, M. Park, L. Zhou, G.-H. Lee, J. Shin, Z. Hu, S.-L. Chou, J. Chen and Y.-M. Kang, *Angew. Chem. Int. Ed.*, 2016, **55**, 12822-12826.·

7 W. Chen, S. Qi, L. Guan, C. Liu, S. Cui, C. Shen and L. Mi, *J. Mater. Chem. A*, 2017, **5**, 5332-5341.·

8 Z. Lu, N. Wang, Y. Zhang, P. Xue, M. Guo, B. Tang, Z. Bai and S. Dou, *Electrochim. Acta*, 2018, **260**, 755-761.·

9 W. Chen, S. Qi, M. Yu, X. Feng, S. Cui, J. Zhang and L. Mi, *Electrochim. Acta*, 2017, **230**, 1-9.·